Equivalent Circuit Modeling of a Multilayer Planar Winding Array Structure for Use in a Universal Contactless Battery Charging Platform

Xun Liu, *Student Member, IEEE*, and S. Y. Ron Hui, *Fellow, IEEE*

***Abstract*—In this paper, an equivalent circuit model of a multilayer planar winding array structure that can be used as a universal contactless battery charging platform is presented. This model includes the mutual-inductive effects of partial overlaps of planar windings in the multilayer structure. It has been successfully simulated with PSpice and practically verified with measurements obtained from three prototypes. This circuit model forms the basis of an overall system model of the planar charging platform. It is demonstrated that model parameters can be derived from the geometry of the winding structure. Errors between the calculated and the measured results are found to be within a tolerance of 5%.**

***Index Terms*—Battery charger, equivalent circuit model, planar spiral inductance.**

I. Introduction

PLANAR contactless battery charging platform is an emerging technology that has the potential of unifying the charging protocols of portable consumer electronic products such as mobile phone, CD players, etc. Recently, two approaches have been proposed and are documented in several patent documents [1], [2], [10]. The first approach [1] adopts a "horizontal flux" approach in which the line of magnetic flux flows horizontally to the planar charging surface. This "horizontal flux" principle is in fact similar to that of the ac electromagnetic flux generated in a cylindrical motor, except that the cylindrical structure is compressed into a flat pancake shape. As the flux needs to flow horizontally along the upper and lower surfaces, two inherent limitations arise. First, an electromagnetic flux guide must be used to guide the flux along the bottom surface. This is usually a layer of soft magnetic material such as ferrite or amorphous alloy. In order to provide sufficient flux, this layer must be "thick" enough so that the flux can flow along the layer of soft magnetic material without magnetic saturation. Second, a similar problem applies to the secondary device that has to pick up the flux (and energy) on the upper surface of the charging platform. Fig. 1(b) shows the energy-receiving device required for the charging platform of Fig. 1(a). It consists of a magnetic core and a winding. In order for the winding to sense the ac flux, the flux must flow into the cross-sectional area [shaded in Fig. 1(b)] that is vertical to the charging surface. Therefore, this cross-sectional area must be large enough (thick and wide enough) so that enough flux and energy can be picked up by the secondary device. It should be noted that this secondary device must be housed inside the electronic equipment to be charged on the charging platform. The thickness of the secondary device is crucial to the applicability and practicality of the device. If it is too thick, it simply cannot be housed inside the electronic equipment.

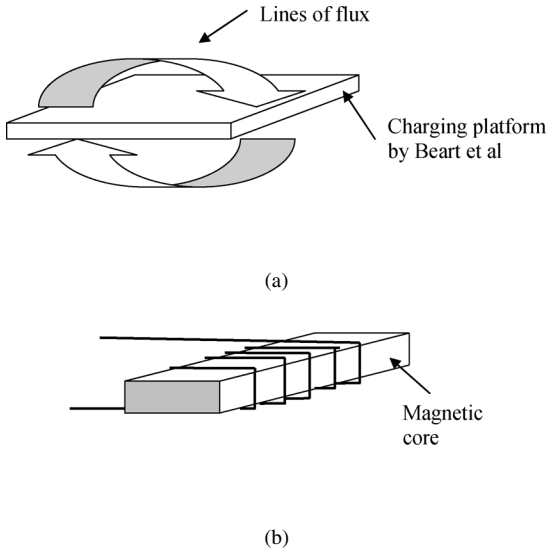

Fig. 1. (a) Inductive battery charging platform (with magnetic flux lines flow "horizontally" along the charging surfaces) proposed by Beart *et al* [1]. (b) Secondary device for use with the charging platform proposed by Beart *et al* [1]. The horizontal flux has to go through the shaded cross-sectional area.

Another planar inductive battery charging platform based on a "perpendicular flux" approach was proposed in [2]. Unlike the one described in [1], this charging platform generates an ac flux that has almost uniform magnitude over the entire charging surface. The lines of flux of this charging platform flow "perpendicularly" into and out of the charging surfaces (Fig. 2). This perpendicular flow of flux is very beneficial to the slim design of the energy-receiving element because it allows the energy transfer over the surface on which the electronic equipment (to be charged) is placed [3]. Particularly, it allows a "thin" secondary energy-receiving device to be developed for the charging

Manuscript received January 24, 2006; revised March 29, 2006. This work was supported by the Hong Kong Research Grant Council under Project CityU 1223/03E and by the City University of Hong Kong. Recommended for publication by Associate Editor J. A. Ferreira.

The authors are with the Department of Electronic Engineering, City University of Hong Kong, Hong Kong, China (e-mail: eeronhui@cityu.edu.hk).

Color versions of one or more of the figures in this paper are available online at http://ieeexplore.ieee.org.

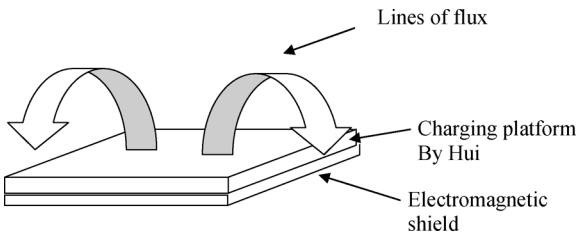

Fig. 2. Inductive battery charging platform (with magnetic flux lines flowing in and out perpendicularly of the charging surface) proposed by Hui [2].

Fig. 3. Photograph of a universal planar charging platform [5].

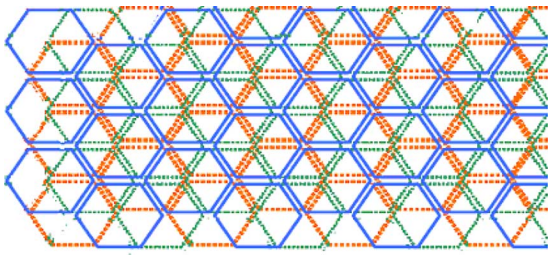

Fig. 4. Structure of three-layer hexagonal-spiral PCB winding arrays to generate uniform MMF over the planar surface.

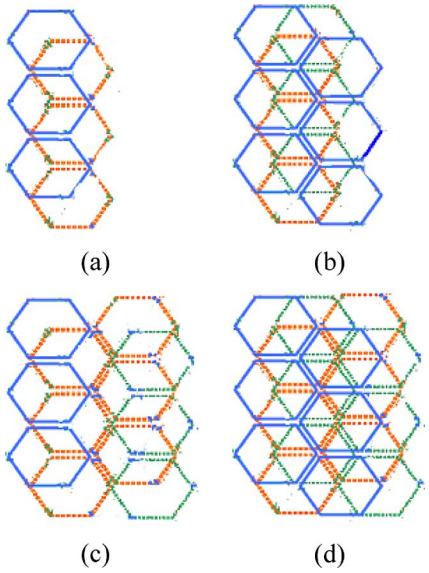

Fig. 5. Structure of the combination of different columns.

TABLE I
GEOMETRY OF EACH WINDING OF THE THREE PLATFORMS

Platform	Number of turns, n	Outer diameter, d_{out} (mm)	Track width, w (mm)	Spacing between tracks, s (mm)
A	25	36.2	0.45	0.25
B	16	36.2	0.74	0.36
C	22	49.5	0.84	0.26

For both planar charging platforms described above, it is necessary to use an electromagnetic shield on the bottom surface. In case the charging platform is placed on a metallic desk, the ac flux generated in the charging platform may induce currents in the metallic desk, resulting in incorrect energy transfer and even heating effects in the metallic desk. A patented electromagnetic shield [4] has been shown to be effective for this type of planar charging platform. The electromagnetic shield in patent [4] simply consists of a thin layer of soft magnetic material (such as ferrite) and a thin layer of conductive material (such as copper).

Based on the "perpendicular flux" approach, we focus on a contactless battery charging platform for portable consumer electronic equipment (Fig. 3). In [2], [3], and [5], the fundamental principles of the uniform magnetomotive force (MMF) generation based on multilayer printed circuit board (PCB) winding arrays were illustrated and verified by experiments. By representing a spiral hexagonal planar winding as a single hexagon, the structure of the three-layer hexagonal-spiral PCB winding arrays is shown in Fig. 4. Each layer of winding array is represented by a different color (red, blue and green).

Fig. 5 shows a few combinations of the overlapped multi- in Fig. 5(a)] are considered as one "column" of windings. Each hexagonal winding spirals inwardly. The winding ends in the center of the hexagon and then moves into another layer as the beginning of another hexagonal winding. It can be seen that there is some overlap of the hexagonal windings even within each column. Fig. 5(b) shows the structure of two adjacent columns. Since there is overlap between them, they are considered to be "overlapped" columns. Fig. 5(c) shows that there is no overlap between the first and third columns. So they are considered to be "nonoverlapped" columns. In this paper, the equivalent circuit model is developed by considering the inductance of one column of six series-connected hexagonal windings as one unit (or column) of the multilayer winding structure. Attention is paid to the negative coupling effects between the overlapped and non-overlapped windings and columns. To verify the circuit model, the measured and simulated input impedance are compared. This equivalent circuit modeling of the multilayer planar winding arrays forms the basis of the overall modeling of the charging platform. If the parameters of the circuit model could be calculated based on the dimensions and geometry of the winding array structure

TABLE II
CALCULATED, SIMULATED AND MEASURED INDUCTANCE OF ONE WINDING OF THE THREE PLATFORMS

Platform	Measured (μH)	Calculated (μH)	Error	Simulated (μH)	Error
A	9.26	9.29	0.32%	9.13	1.40%
B	3.92	4.00	2.00%	3.85	1.79%
C	9.56	9.75	1.95%	9.42	1.46%

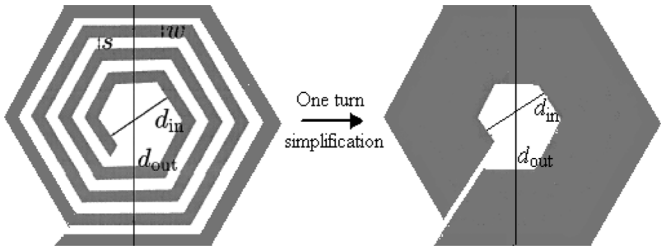

Fig. 6. Configuration of the hexagonal winding [8].

in the early design stage. From previous research [6]–[8], the inductance of each hexagonal spiral winding can be calculated from the geometry of the spiral winding. The mutual effects between the windings can be simulated out quickly by the use of the simplified one-turn model. Based on the calculated and simulated results, inductive parameters of the circuit model could be estimated, and the optimal operating frequency of the charging platform can be decided. The resistive parameters of the circuit model can also be calculated using the skin effect equations so that the power loss of the planar winding arrays can be predicted. The equivalent circuit model with the parameter estimation provides a useful tool not only for performance prediction but also for initial design of the charging platform.

II. CIRCUIT MODELING OF THE MULTILAYER PLANAR WINDING ARRAYS

In this study, three planar three-layer PCB winding array structures (or platforms) are used to evaluate the validity of the equivalent circuit. The three prototypes have eight, eight, and six columns, respectively. Structural details of each hexagonal winding unit of the three prototypes are given in Table I. The meaning of the parameters in Table I, d_{out}, w, and s is illustrated in Fig. 6.

A. Inductance of one Column

The configuration of one hexagonal winding is shown in Fig. 6. The hexagonal winding and the winding array can not be revolved around an axis of symmetry, so that their inductance can not be computed directly by the use of the relatively easier and quicker 2-D finite element simulator in Ansoft [9]. The 3-D field simulator in Ansoft is an available replacement. But such computation is very time-consuming and is more appropriate for design verification than the design of an inductor. is another alternative, which uses multipole-acceleration to reduce both required memory and computation time so that the complexity grows more slowly with problem size. It will be used as a reference in the later part.

On the other hand, the more efficient way for self-inductance calculation is to consider some analytical methods. The Hurley method [6] takes full account of the current density distribution in the coil cross section and the eddy current losses in the substrate, which makes it adequately precise. But the formulas are based on the equation of the mutual inductance between two circular filaments. So when it is used to calculate the hexagonal inductors, some approximation must be made in advance. With the increase of the number of turns, such approximation may accumulate to a potential error. Another technique is to use the Greenhouse method [7] to calculate the inductance. The Greenhouse method offers sufficient accuracy and adequate speed, but cannot provide an inductor design directly from specifications and is cumbersome for initial design. Reference [8] provides three new approximation expressions for the inductance of square, hexagonal, octagonal, and circular planar inductors. The third expression in [8] is obtained by using data-fitting techniques, so that it is only applicable to inductors in the author's database. By comparing the first two expressions, the second one considers the concepts of geometric mean distance (GMD), which makes it more suitable for the PCB tracks with rectangular cross sections. Comparison between the calculated results with the simulated and measured results also shows that the second expression can achieve an accuracy high enough. The self-inductance of one winding is expressed by the second method in [8] as

$$L_w = \frac{\mu n^2 d_{\text{avg}} c_1}{2}\left(\ln(c_2/\rho) + c_3\rho + c_4\rho^2\right) \tag{1}$$

where n is the number of turns, d_{avg} is the average diameter and equals $0.5(d_{\text{out}} + d_{\text{in}})$, ρ is the fill ratio and defined as $\rho = (d_{\text{out}} - d_{\text{in}})/(d_{\text{out}} + d_{\text{in}})$, d_{out} and d_{in} are illustrated in Fig. 6, and c_1–c_4 are 1.09, 2.23, 0.00, and 0.17, respectively, for hexagonal winding.

With the use of (1), the inductance values of one winding of the three platforms are calculated and compared with the measured results, as listed in Table II. The simulated results by the use of FastHenry are also presented. The errors are not higher than 2%.

As shown in Fig. 5(a), six windings are connected in series to form a column, with some overlaps. Similarly, as explained in

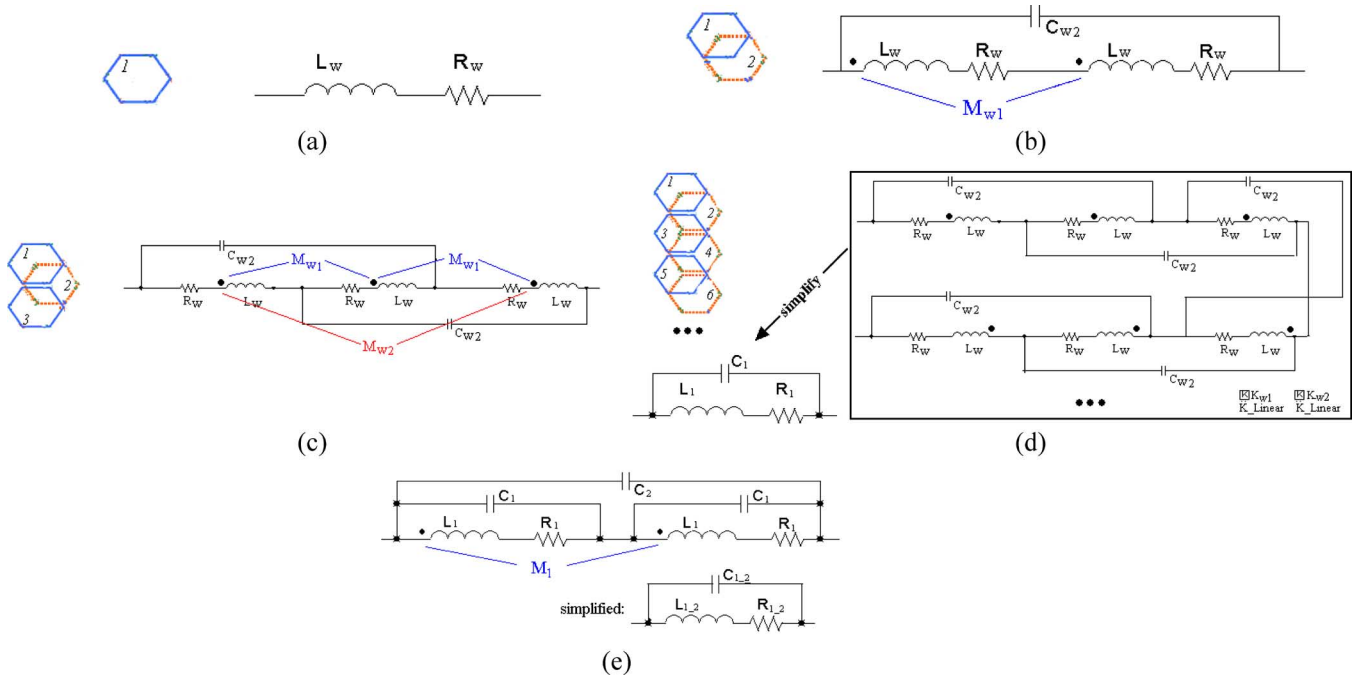

Fig. 7 Equivalent circuit of (a) one winding, (b) two adjacent windings, (c) three adjacent windings, (d) one single column, and (e) two adjacent columns.

one column is definitely a portion of the sum of the self-inductance of the six windings. Fig. 7(a) shows the circuit model of one winding. It consists of a resistor (R_w) and an inductor (L_w) connected in series. When two partly-overlapped windings are considered, as shown in Fig. 7(b), the mutual inductance between them, $M_{\rm w1}$, must be included. The mutual coupling coefficient, $K_{\rm w1}$ which is equal to $M_{\rm w1}/L_{\rm w}$ numerically, can be calculated out by fully modeling it in finite element software. But even with the accelerated method, such as using FastHenry, the required memory and computation time still grow faster than n, where n is the number of volume-elements [11]. This problem becomes much more serious when the coupling effects between columns are considered later in the paper. In [12], it is demonstrated that the mutual coupling coefficient between windings can be approximated out by simplifying each winding into one turn with the same dimension, as shown in Fig. 6. From [12], a conclusion can be extended that such approximation is accurate enough only if the spacing between tracks is smaller than the track width, $s < w$. Such condition is always desired and satisfied in this design because a smaller spacing improves the inter-winding magnetic coupling and reduces the power loss [8]. For three adjacent windings as shown in Fig. 7(c), the mutual coupling coefficient between two nonoverlapped windings is represented by $K_{\rm w2}$ which equals $M_{\rm w2}/L_{\rm w}$. Its value can also be simulated out quickly with the one-turn winding structure. $C_{\rm w2}$ models the capacitive coupling between the overlapped areas. It is in the order of only a few tens of pico-Farads. Fig. 7(d) shows the detailed equivalent circuit of one single column which consists of six windings or more connected in series. For simplicity, $K_{\rm w1}$ and $K_{\rm w2}$ are represented by two PSpice K_Linear parts in the figure. The inductance of one single column, L_1, is approx-

where m is the number of windings connected in series to form a column. Derivatoin of (2) is given in the Appendix.

The simulated values of $K_{\rm w1}$ and $K_{\rm w2}$ by the use of the simplified one-turn winding structure are listed in Table III. It can be found that the coupling coefficients between the windings of Platform A and B are the same because they have the same dimensions. In addition, the simulated value of the coupling coefficients between "far-apart" windings ($K_{\rm w3}$, $K_{\rm w4}$, etc.) shows that they are small enough to be neglected. The self-inductance of one column of the three platforms are calculated with (2) and compared with the measured results in Table III. In the calculation, the calculated inductance of one winding as listed in Table II is used. The agreement between the calculated and measured results proves the accuracy of such one turn simplification for coupling calculation.

B. Mutual Effects Between Columns

The equivalent circuit of one single column and two adjacent columns are shown in Fig. 7(d) and (e). L_1, C_1 and R_1 represent the inductance, capacitance, and resistance of one column, respectively. In Fig. 7(e), C_2 represents the capacitance between two adjacent columns. The circuit model can be easily implemented in PSpice. The PSpice K_Linear part, K_1 represents the mutual inductance (M_1) between two adjacent columns [e.g., columns 1 and 2, or columns 2 and 3, or columns 3 and 4, etc. as shown in Fig. 5(b)]. Numerically, K_1 equals M_1/L_1. Fig. 7(e) also shows the simplified equivalent circuit of two adjacent columns. The overall inductance, resistance, capacitance of m (where $m = 2,3,\ldots 8$) series-connected columns are defined as L_{1_m}, R_{1_m}, and C_{1_m}, respectively.

TABLE III
CALCULATED AND MEASURED INDUCTANCE OF ONE COLUMN OF THE THREE PLATFORMS

Platform	K_{w1}	K_{w2}	Calculated (μH)	Measured (μH)	Error
A	-0.04670	-0.02625	49.45	51.45	3.89%
B	-0.04670	-0.02625	21.29	21.10	0.90%
C	-0.05135	-0.02802	51.31	50.77	1.06%

TABLE IV
CALCULATED AND MEASURED INDUCTANCE OF TWO COLUMNS OF THE THREE PLATFORMS

PLATFORM	K_1	Calculated(μH)	Measured(μH)	Error
A	-0.1663	82.45	86.86	5.08%
B	-0.1663	35.50	35.20	0.85%
C	-0.1666	85.52	83.90	1.93%

TABLE V
CALCULATED AND MEASURED INDUCTANCE OF THREE COLUMNS OF THE THREE PLATFORMS

PLATFORM	K_2	Calculated(μH)	Measured(μH)	Error
A	-0.06845	108.70	113.90	4.56%
B	-0.06845	46.80	46.20	1.30%
C	-0.06750	112.80	109.65	2.87%

of two series-connected adjacent columns (such as columns 1 and 2) can be expressed as

$$L_{1\_2} = 2L_1 + 2M_1 = (2 + 2K_1)L_1 \tag{3}$$
$$R_{1\_2} = 2 * R_1 \tag{4}$$
$$C_{1\_2} = \frac{C_1}{2} + C_2. \tag{5}$$

From (3), the mutual inductance between two adjacent columns is

$$M_1 = \frac{L_{1\_2} - 2L_1}{2}. \tag{6}$$

L_1, C_1, R_1, L_{1_2}, C_{1_2}, and R_{1_2} can be measured with an impedance analyzer (HP4194A), or be determined from the dimensions and geometry of one winding column. To determine the value of K_1, the one-turn simplification method is also used. In the simulation, each column is simplified to six one-turn windings connected in series so that the required memory and computation time decrease obviously. The simulated K_1 of the three platforms is listed in Table IV. It is found interestingly that K_1 is almost a fixed value for the three platforms. The calculated inductance of two adjacent columns of the three platforms by the use of (3), as well as the measured results is also given

When the inductance of three adjacent columns as shown in Fig. 5(d) is taken into account, the mutual inductance M_2 between the "two nearest" nonoverlapped columns [columns 1 and 3, or columns 2 and 4, or columns 3 and 5, etc. as shown in Fig. 5(c)] should be considered. Another K_Linear part, K_2 represents the mutual inductance (M_2) between the "two nearest" non-overlapped columns. It is equal to M_2/L_1 numerically. The inductance of columns 1, 2 and 3 connected in series, L_{1_3} can be expressed as

$$L_{1\_3} = 3L_1 + 4M_1 + 2M_2 = (3 + 4K_1 + 2K_2)L_1. \tag{7}$$

The mutual inductance, M_2 is

$$M_2 = \frac{L_{1\_3} - 3L_1 - 4M_1}{2}. \tag{8}$$

Similarly, the simply simulated K_2 is listed in Table V. It can be found that the difference between the three platforms is very small too. The calculated inductance of three columns and the measured results are also given out. The agreement between the calculated and measured results in Table IV and V proves that such one-turn simplification is also applicable for the calculation of coupling effects between columns.

The negative sign of mutual inductance can be explained by the definition of mutual inductance. Let us use two adjacent

DOCKET ALARM

Explore Litigation Insights

Docket Alarm provides insights to develop a more informed litigation strategy and the peace of mind of knowing you're on top of things.

Real-Time Litigation Alerts

Keep your litigation team up-to-date with **real-time alerts** and advanced team management tools built for the enterprise, all while greatly reducing PACER spend.

Our comprehensive service means we can handle Federal, State, and Administrative courts across the country.

Advanced Docket Research

With over 230 million records, Docket Alarm's cloud-native docket research platform finds what other services can't. Coverage includes Federal, State, plus PTAB, TTAB, ITC and NLRB decisions, all in one place.

Identify arguments that have been successful in the past with full text, pinpoint searching. Link to case law cited within any court document via Fastcase.

Analytics At Your Fingertips

Learn what happened the last time a particular judge, opposing counsel or company faced cases similar to yours.

Advanced out-of-the-box PTAB and TTAB analytics are always at your fingertips.

API

Docket Alarm offers a powerful API (application programming interface) to developers that want to integrate case filings into their apps.

LAW FIRMS
Build custom dashboards for your attorneys and clients with live data direct from the court.

Automate many repetitive legal tasks like conflict checks, document management, and marketing.

FINANCIAL INSTITUTIONS
Litigation and bankruptcy checks for companies and debtors.

E-DISCOVERY AND LEGAL VENDORS
Sync your system to PACER to automate legal marketing.